KH-type splicing regulatory protein controls colorectal cancer cell growth and modulates the tumor microenvironment

Francesco Caiazza[*1,2,8], Katarzyna Oficjalska[1,2], Miriam Tosetto[1], James J. Phelan[3], Sinéad Noonan[1], Petra Martin[1], Kate Killick[4], Laura Breen[5], Fiona O'Neill[5], Blathnaid Nolan[1], Simon Furney[6], Robert Power[2,7], David Fennelly[1,2], Charles S. Craik[8], Jacintha O'Sullivan[3], Kieran Sheahan[1,2], Glen A. Doherty[1,2] and Elizabeth J. Ryan[1,2]

[1]Centre for Colorectal Disease, St. Vincent's University Hospital, Elm Park, Dublin, Ireland. [2]School of Medicine, University College Dublin, Ireland. [3]Trinity Translational Medicine Institute, Department of Surgery, Trinity College Dublin, Ireland. [4]Systems Biology Ireland, University College Dublin, Ireland. [5]National Institute for Cellular Biotechnology, Dublin City University, Ireland. [6]Department of Physiology and Medical Physics, Royal College of Surgeons in Ireland. [7]Personalis Inc., Menlo Park, California, U.S.A. [8]Department of Pharmaceutical Chemistry, University of California San Francisco, San Francisco, U.S.A.

*Corresponding author: Francesco Caiazza, Department of Pharmaceutical Chemistry, University of California San Francisco, 600 16th street, Room S-514, San Francisco, California, U.S.A. francesco.caiazza@gmail.com.

Short title: Role of KHSRP in colorectal cancer

Financial Support: This work was supported by a Newman Fellowship awarded by the UCD Foundation to FC funded by a donation from Merck Serono, from a Science Foundation Ireland Industry Fellowship (14/IFB/2715) to FC, NIH P41CA196276 to CSC and from the Irish Health Research Board (HRA _POR_2013_281) to EJR. The sponsors had no role in the study design, collection, analysis, or interpretation of data.
Conflict of Interest: The authors declare no potential conflicts of interest
Authors contribution: Study concept and design: FC, EJR, JOS, GAD; acquisition of data: FC, KO, MT, LB, FON, RP, SN, PM; analysis and interpretation of data: FC, KO, JP, KK, SF, KS, JOS, EJR; drafting and critical revision of the manuscript: FC, KO, JOS, EJR, CSC; funding and support: EJR, KS, GAD, DF, CSC; administrative, technical or material support: MT, BN; study supervision: EJR, GAD.
Word count: 3725 (excluding abstract, methods, reference and legends)
Total number of figures: 7, **Total number of tables:** 1

Abbreviations: KHSRP, KH-type splicing regulatory protein; CRC, colorectal cancer; IHC, immunohistochemistry; FFPE, formalin fixed paraffin embedded; RBP, RNA-binding protein; UTR, untranslated region; ARE, AU-rich element; TCGA, The cancer genome atlas; DAMP, damage-associated molecular pattern; PAMP, pathogen-associated molecular pattern.

Synopsis:

Here we describe a pro-tumorigenic role for KHSRP in colorectal cancer. Higher KHSRP expression is associated with shorter overall survival. KHSRP regulates cancer cell proliferation and expression of proteins that govern processes including angiogenesis, migration and response to cellular stress.

ABSTRACT

Background & Aims: KH-type splicing regulatory protein (KHSRP) is a multifunctional nucleic acid binding protein. KHSRP regulates transcription, mRNA decay and translation, and miRNA biogenesis. These distinct functions are associated with key aspects of cancer cell biology: inflammation and cell-fate determination. However, the role KHSRP plays in colorectal cancer (CRC) tumorigenesis remains largely unknown.

Methods: We investigated the oncogenic role of KHSRP in CRC using a combination of *in silico* analysis of large datasets, *ex vivo* analysis of protein expression in patient samples, and mechanistic studies using *in vitro* models of CRC.

Results: KHSRP was expressed in the epithelial and stromal compartments of both primary and metastatic tumors. Elevated KHSRP expression was found in tumor versus matched normal tissue in a cohort of 62 patients. This finding was validated in larger independent cohorts *in silico*. KHSRP expression was a prognostic indicator of worse overall survival (HR=3.74, 95% CI = 1.43-22.97, p=0.0138). Mechanistic data in CRC cell line models supported a role of KHSRP in driving epithelial cell proliferation in both a primary and metastatic setting, through control of the G1/S transition. Additionally, epithelial KHSRP was involved in promoting a pro-angiogenic extracellular environment, as well as regulating the secretion of oncogenic proteins involved in diverse cellular processes such as migration and response to cellular stress.

Conclusion: Our study has uncovered novel mechanistic-based data on the tumor-promoting effects of KHSRP in CRC.

Keywords: RNA-binding protein; prognostic biomarkers, inflammation, cell cycle

INTRODUCTION

The dysregulation of mRNA translation is a crucial attribute of the transformed phenotype. Sustained proliferation, one of the hallmarks of cancer[1], requires increased rates of global protein synthesis, which are achieved through alterations in the expression and activity of specific translation factors, as well as increased ribosome biogenesis and recruitment[2]. Reprogramming of translation is controlled by almost all the major oncogenic signaling pathways, affecting cancer initiation and progression by directing selective translation of specific tumor-promoting mRNAs[3]. Regulation of transcript-specific translation involves RNA-binding proteins (RBP) capable of recognizing sequence-specific regulatory elements in the 3'UTR, that promote mRNA splicing, stability and translation[4].

The KH-type splicing regulatory protein (KHSRP, also known as KSRP or FUBP2) is a RBP which binds to mRNA containing an AU-rich element (ARE), the major *cis* regulatory element responsible for rapid mRNA decay in mammalian cells. AREs are found in the 3′UTRs of short-lived transcripts, such as those encoding cytokines, chemokines, transcription factors, proto-oncogenes, and cell-cycle regulators[5]. KHSRP regulates translation by mediating mRNA decay through direct binding and recruitment of proteins involved in RNA degradation, including the Poly(A)-Specific Ribonuclease (PARN), exosome components and decapping enzymes[6,7]. Alternatively, KHSRP can regulate translation independently of mRNA decay, either by promoting translational inhibition[8] or indirectly by promoting maturation of selected miRNA precursors[9]. Adding a further layer of complexity, KHSRP also acts as a transcription factor, inducing the expression of the *MYC* oncogene[10].

The KHSRP-mediated control of mRNA translation and stability has been extensively studied in the context of innate immunity[8,11]. Key pro-inflammatory cytokines and chemokines (e.g. IL-6, IL-8, TNF-α, IL-1β), as well as other inflammatory mediators (iNOS and c-fos) are directly targeted and negatively regulated by KHSRP[5,12]. Consequently, *Khsrp*$^{-/-}$ mice are capable of mounting an increased type I interferon (IFN) response and are more resistant to viral infection[13]. However, it is likely that the role of

KHSRP is cell type and context dependent, with the balance between KHSRP and other RBP with similar or divergent regulatory effects an important consideration[14].

In recent years direct evidence for the involvement of KHSRP in cancer has been accumulating. KHSRP contributes to maintaining P19 mouse teratocarcinoma cells in a undifferentiated stem cell-like state, while its knockdown promotes neural differentiation[15]. KHSRP has a multi-faceted role in breast cancer pathogenesis. First of all, KHSRP expression is regulated by the breast cancer susceptibility gene 1 (BRCA1), and BRCA1 mutated tumors overexpress KHSRP[16]. Additionally, the mutant p53-dependent regulation of the aggressive phenotype of triple negative breast cancer is dependent on proteasome-mediated destabilization of KHSRP, and subsequent deregulation of oncosuppressive miRNAs such as let-7a and miR-30c[17]. Furthermore, KHSRP is involved in the TGF-β-dependent regulation of epithelial-to-mesenchymal transition in the mammary gland[18]. Finally, KHSRP has also been implicated in the pathogenesis of small cell lung cancer[19] and osteosarcoma[20]. There is additional indirect evidence to suggest that KHSRP has pleiotropic roles in tumorigenesis, for example through regulation of lipid metabolism or mediating the cellular response to DNA damage[12].

The role of KHSRP in cancer, however, remains underappreciated, unlike that of other RBPs such as HuR and the cytoplasmic polyadenylation element-binding (CPEB)[21]. This is particularly true in the context of colorectal cancer (CRC): while other RBPs have been involved in cellular transformation in the intestinal epithelium (namely, ESRP1[22], Apobec-1[23], Musashi (MSI)-1[24], and MSI-2[25]), KHSRP remains largely under-investigated in this indication. Interestingly, adenomatous polyposis coli (APC), a tumor suppressor frequently mutated in CRC, is itself a RBP capable of regulating the translation of mRNAs associated with cell adhesion, motility and other cellular processes crucial for carcinogenesis[26], suggesting the importance of RBP-mediated translation control in the gut. Here we use a combination of bioinformatic, *in vitro* and *ex vivo* approaches to dissect the role of KHSRP in both regulation of cell proliferation and

inflammatory environment in CRC and provide evidence for a novel prognostic role of the RBP in intestinal tumorigenesis.

MATERIALS AND METHODS

Bioinformatic analysis of publicly available datasets

CRC datasets in the Oncomine database (www.oncomine.org, 11/2014 version, Thermo Fisher Scientific, Ann Arbor, MI) were searched using the differential expression module for cancer vs. normal tissue; output of the resulting database searches was downloaded for offline plotting, along with detailed gene expression results for 2 representative cohorts (GSE9348 and TCGA). A similar analysis was conducted without restricting for cancer type. Differential expression analysis of RNA-Seq data for 12 tumor-normal pairs in the TCGA database was previously described and made available by the authors[27]. The RNA-Seq expression and the frequency of genetic alterations for KHSRP in the TCGA cohort were analyzed using the cBio portal (www.cbioportal.org)[28]. All other datasets were downloaded from the Gene Expression Omnibus (https://www.ncbi.nlm.nih.gov/geo/), using the indicated accession number.

Patient Samples and Tissue Microarrays

Ethical approval to conduct all aspects of this work was granted by the Research and Ethics Committee of St. Vincent's University Hospital. Fresh-frozen tumor and adjacent normal tissue samples were obtained from 16 patients and were used for protein isolation and Western blotting (WB cohort) as described thereafter. Tissue microarrays (TMA) were accessed from a previously described cohort of formalin-fixed paraffin-embedded (FFPE) archival resected tumor tissue samples[29]. Patient details for both cohorts are reported in Table 1. For immunohistochemistry, TMA sections were incubated with a 1:250 dilution of a rabbit polyclonal anti-KHSRP antibody (HPA034739, Sigma-Aldrich, Saint Louis, MO, USA), and secondary antibody horseradish peroxidase (DAKO Agilent, Santa Clara, CA, USA). Endogenous peroxidase activity was blocked using 3% hydrogen peroxide, and non-specific binding was blocked with casein buffer. Diaminobenzidine was used to visualize staining and sections were counter-stained with haematoxylin, dehydrated and mounted. Stained TMA sections were acquired with a ScanScope XT high throughput scanning system (Aperio Technologies, Leica Biosystems, Buffalo Grove, IL, USA) and images were scored by two independent investigators, blinded to

the clinical data. Both epithelial and stromal cells were assessed for staining intensity and percent positivity; positive cell count was scored as a continuous variable (0-100%), while intensity was scored using a scale of 0 to 3 (correlating with negative, weak, medium and strong staining, respectively). The mean value of each parameter from the two investigators was calculated, and parameters were averaged from all tissue cores related to the same patient; the two parameters were finally combined using the semi-quantitative *quickscore* method[30]. There was a good correlation between the two assessors (weighted Cohen Kappa coefficient = 0.63).

Cell Culture and gene knockdown

SW480 and SW620 cells were obtained from the American Tissue Culture Collection and maintained in DMEM supplemented with 10% fetal bovine serum, 1% penicillin/streptomycin and 1% Fungizone (all from Invitrogen Life Technologies, Carlsbad, CA, USA). Cell line identity was confirmed by analysis of Short Term Repeat loci, and cells were routinely tested for mycoplasma infection. Cells were seeded in 24-well plates to be transfected with 30 pmol KHSRP siRNA (Silencer Select, Thermo Fisher) or non-targeting scramble siRNA using 2 µl Lipofectamine 2000 (Invitrogen) for 48h. Alternatively, cells were transfected with 50 nM KHSRP siRNA (SMARTpool: ON-TARGET plus) and corresponding Non-Targeting Pool (Dharmacon, Lafayette, CO, USA).

Protein isolation, immunoblotting, immunofluorescence and ELISA

Cells or tissue homogenate were lysed in RIPA buffer (150 mM NaCl, 50 mM Tris-HCl, 1% Triton, 0.5% sodium deoxycholate, 0.1% SDS) supplemented with a protease and phosphatase inhibitor cocktail (Roche Applied Science, Burgess Hill, UK) and 1 mM PMSF (Sigma Aldrich). Total protein concentration was determined using the BCA Protein Assay Kit (Thermo Scientific Pierce, Waltham, MA, USA). Total proteins (10-20µg) were separated on 10% SDS–PAGE gels and wet-transferred to PVDF using the mini-PROTEAN® TGX™ system (BioRad, Hercules, CA, USA). Membranes were pre-blocked with 5% low-fat dry milk in TBS-T and incubated with a rabbit polyclonal anti-KHSRP antibody (Sigma-Aldrich) and anti-rabbit (Cell Signaling, Danvers, MA, USA)

horseradish peroxidase-conjugated secondary antibody. Proteins were visualized by chemiluminescence with ECL substrate (Thermo Scientific Pierce) and semi-quantified using ImageJ software (US National Institute of Health, Bethesda, MD, USA; http://imagej.nih.gov/ij/) with normalization against β-actin (Sigma-Aldrich). Cells were fixed on chamber slides with 4% Formaldehyde, permeabilized with 0.5% Tween in PBS, and immunofluorescence was performed using a Cy3-anti-rabbit, DAPI and Phalloidin counter-stain (DAKO) on a Leitz DM40 microscope (Leica Microsystems) equipped with the AxioCam system and AxioVision 3.0.6 for image acquisition. Human interleukin-8 and vascular endothelial growth factor (VEGF) were quantified in cell culture supernatants using DuoSet® ELISA (R&D Systems, Minneapolis, MN, USA), following manufacturer's instructions.

RNA isolation and qRT-PCR

Total RNA was isolated from cells using the EZNA Total RNA Kit (Omega, VWR, Radnore, PA, USA). 1 µg of RNA was reverse-transcribed into cDNA using the RT Omniscript cDNA kit (Qiagen, Germantown, MA, USA), and 20 ng of cDNA template was amplified on a LightCycler-480 (Roche, Indianapolis, IL, USA) using a FAST SYBR Green Master Mix (Invitrogen) under the following conditions: pre-incubation step at 95 °C for 5 min was followed by 45 cycles of denaturation at 95 °C for 10 sec, annealing at 60 °C for 10 sec, and elongation at 72 °C for 10 sec. GAPDH was used as the housekeeping gene. The mRNA expression levels of all samples were normalised to the housekeeping gene and calculated using the delta Ct method. The following primers were used in qPCR: KHSRP Forward: 5'-CCGCTTACTACGGACAGACC-3';
KHSRP Reverse: 5'-ATTCATTGAGCCTGCTGCTGT-3';
GAPDH Forward: 5'-CGGATTTGGTCGTATTGGGCGCCTG-3';
GAPDH Reverse: 5'-CAGCATCGCCCCACTTGATTTTGGA-3'.

Cell-based assays

Cell proliferation was measured by Neutral Red (NR) staining[31]. Real-time cell proliferation was measured using an E-plate 16 (RTCA DP Analyser, xCelligence System, Roche) following the manufacturer's protocol. Cells were seeded at 10,000 cells/well and the recording of the Cell Index (CI) occurred every 15 min during the first six hours, and every hour for the rest of the period. Cells seeded at low density for colony-formation assay were fixed in methanol/citric acid (4:1 v/v), stained in 2% crystal violet and counted with ImageJ. Plating efficiency was calculated by dividing the number of colonies by the original seeding density. The surviving fraction was determined by comparing the plating efficiency of transfected vs control wells. The total colony area was calculated for each biological replicate by averaging the area of all colonies in replicate wells. Spheroids were cultured on Matrigel following the 3D on-top protocol[32], stained with NR and quantified via ImageJ. Scratch-wound assays were performed in culture inserts 2-well μ-dishes (Ibidi, Martinsried, Germany), quantified with ImageJ (MiToBo plugin) and representative images prepared with WimScratch (Ibidi). Invasion assays were performed using Matrigel-coated Boyden chambers (8-μm pore size; BioCoat, BD Biosciences, Erembodegem-Dorp, Belgium) for 72h against 10% FBS as chemo-attractant. Invaded cells were fixed using 1% glutaraldehyde, stained with 0.1% crystal violet, and imaged with a light microscope at a 10X magnification, averaging five random fields per insert. Crystal violet staining was quantified with ImageJ. Endothelial HDEC cells were seeded on Matrigel in MCDB131 medium with 40% conditioned medium from SW620 cells. Tubes were manually counted after 6h, and images prepared with WimTube (Ibidi).

Flow Cytometry

Cell cycle analysis was carried out by propidium iodide (PI) staining. Cells were resuspended at 1-2x10^6 cells/ml in PBS and fixed in 70% ethanol for 2h at -20°C, washed twice in PBS, and re-suspended in staining solution [0.1% (v/v) Triton X-100, 10 μg/mL PI, 100 μg/mL DNase-free RNase A in PBS] for 30' at R.T. Data was acquired on a CyAn ADP (Beckman Coulter) using 488nm excitation laser, and data de-convolution was performed in FlowJo® (Becton Dickinson, Franklin Lakes, NJ, USA). To quantify

the mitotic index, fixed cells were permeabilized with 0.25% Triton X-100 in PBS for 20' on ice, blocked with 10% BSA in PBS and incubated with 1 µg of an Alexa Fluor® 488-conjugated anti-phospho-histone H3 (Ser10) antibody (BioLegend). After washing, cells were re-suspended in PBS containing 50 µg/ml PI for 15' on ice prior to analysis on a CyAn ADP using 488nm excitation laser. Mitotic cells with 4N DNA and elevated levels of phosphorylated histone H3 can be detected by plotting FL1-H versus FL3-A.

Statistics and Data Availability

Statistical significance (p-values) was determined with paired Student's *t*-test or one-way ANOVA for differences between experimental group mean values. Where data required non-parametric statistics, the Wilcoxon signed-rank test or the Mann-Whitney U test were used for paired or unpaired experimental groups (respectively). The statistical test used in each experiment is specified in the relevant figure legends. Survival curves were calculated according to the Kaplan–Meier method and compared using a univariate Cox–Mantel log-rank test. Two-tailed p-values < 0.05 were considered statistically significant. Data are represented as mean ± S.E.M., unless stated otherwise. All analyses were performed using Prism 6 (Graphpad Software, La Jolla, CA, USA) or R Studio open source edition (RStudio, Inc., Boston, MA. http://www.rstudio.com/).

Gene expression microarray data from this study have been deposited in the Gene Expression Omnibus under accession number GSE112329. Raw data from the proteomic analysis is publicly available for download on the MassIVE database (ftp://massive.ucsd.edu/MSV000082206). All authors had access to the full data, and have reviewed and approved the final manuscript.

Additional experimental procedures

The generation of stable conditional knock-down cell lines, the gene expression microarray, and the shotgun proteomics analysis of the cell secretome are described in the supplementary methods.

RESULTS

KHSRP is overexpressed in Colorectal cancer

To profile KHSRP expression in CRC, we performed a meta-analysis of CRC microarray datasets from the Oncomine database (www.oncomine.org). *KHSRP* expression was increased in tumor compared to normal tissue across 18 CRC patient cohorts from 8 different datasets, with a median adjusted p-value of 4.06×10^{-6} (Figure 1-A, and supplementary table 1). *KHSRP* ranked in the top 5% of overexpressed genes in two of these analyses (GSE9348 and GSE6988), and in the top 25% for 8 other analyses. In the remaining 8 analyses *KHSRP* was not one of the most overexpressed genes (<25%). Only 4 of the 17 analyses (from GSE5261 and GSE9689) fell below the threshold of significance. Figure 1-B shows individual data from the GSE9348 cohort[33], in this dataset *KHSRP* expression was increased by 2-fold on average in 70 patients with early stage (stage II) colorectal carcinoma compared to healthy controls ($p=4.6 \times 10^{-11}$). While in the TCGA cohort[34] (also shown in Figure 1-B) *KHSRP* expression increased in 211 samples of colorectal adenocarcinoma (any stage) compared to normal tissue (pooled analysis, +1.36 fold change, $p<0.0001$). In an additional analysis of the GSE6988 cohort[35], *KHSRP* expression increased in samples from either primary colon adenocarcinoma (n=25) or liver metastases (n=13) compared to matched normal colon mucosa and normal liver tissue, respectively (Figure 1 - Supplement 1).

Increased *KHSRP* in tumor tissue was not limited to CRC but remained significant across a meta-analysis of 59 cancer types in Oncomine (median adjusted p-value=0.004, supplementary table 2). In addition, to look at expression of *KHSRP* across different cancer types we utilized RNA-Seq transcriptomic data available in the TCGA database, from which differentially expressed genes were derived for 12 different cancer types against their respective normal tissue[27]: *KHSRP* was significantly overexpressed to varying degrees in 10 cancer types (Figure 1-C), with CRC being among the most highly significant (Fold change overexpression=1.53, FDR-adjusted p-value=5.02×10^{-11}). The colon has also generally a high tissue-specific cancer expression of *KHSRP* across the entire spectrum of cancers represented in the TCGA (Figure 1 - Supplement 2). However, the frequency of genetic alterations (mutations, deletions or amplifications) in *KHSRP* is less than 2% in the CRC TCGA dataset (Figure 1 – Supplement 3), which is low

considering that the three most commonly mutated genes in CRC (APC, TP53 and KRAS) have mutation frequencies of 81%, 60% and 43%, respectively[34]. Collectively, these *in silico* data provided a framework to support additional investigations into the putative role of KHSRP in the pathogenesis of CRC.

KHSRP is a marker of poor prognosis in colorectal cancer

Next, we investigated KHSRP expression in primary tissue samples to confirm our bioinformatic analysis. Protein extracts were obtained from fresh frozen colorectal tumor and normal adjacent tissue following surgical resection. WB analysis revealed a two-fold increased expression (p=0.0009) of KHSRP in stage IV CRC, compared to matched uninvolved (*adjacent normal*) tissue control (Figure 2-A). Analysis of stage II-III patients showed a similar trend (Figure 2 - Supplement 1-A). The KHSRP antibody used for WB (HPA034739, Sigma-Aldrich) detected a single band at ~82 kDa, the predicted size for the protein, confirming the specificity of this antibody.

We then investigated KHSRP expression using immunohistochemistry (IHC) of a tissue microarray (TMA), which contains tumor and normal tissue from a cohort of 62 patients with late stage (III-IV) CRC[29]. Patient characteristics are summarized in Table 1. KHSRP was expressed in both the epithelial and stromal compartments (Figure 2-B); the staining was quantified using a semi-quantitative method, which combines two different scores of the percentage of positive cells and the average intensity of staining. The score values were significantly higher in tumor versus matched normal tissue in both the epithelium and the stroma (Figure 2-B and 2-C). This was mainly due to differences in percentage of positive cells, while the intensity values were similar overall. There were more KHSRP positive cells in the epithelium than in the stroma, making the score significantly lower in the stroma (Figure 2-C), however the increased expression in tumor compared to normal was more prominent in the stroma, with tumor-to-normal ratios significantly higher (Figure 2 - Supplement 1-B). When tumor-to-normal ratios are plotted separately for each patient, the majority of patients have increased KHSRP expression in the tumor compared to matched normal tissue (Figure 2 - Supplement 1-C and D). High KHSRP expression (more than 20% increase in tumor vs. normal) resulted in decreased overall survival (Figure 2-D, HR=3.74, 95% CI = 1.43-22.97, p=0.0138) in a univariate analysis.

Because most of the patients in this cohort have been diagnosed with metastatic disease, relapse-free survival was not included in the analysis. There was also a weak but significant correlation of the KHSRP tumor-to-normal ratio with tumor size in both epithelium (Pearson r=0.43, p=0.0016) and stroma (Pearson r=0.38, p=0.0051).

For a limited number of cases (N=10 patients), data was also available for the corresponding liver metastasis. In both the epithelium and the stroma, the KHSRP score was significantly higher in the metastatic tissue compared to matched normal liver (Figure 2 Supplement 2-A). Overall the metastasis-to-normal ratio was positive for all except one patient, but the difference between metastasis and normal was vastly larger in the stroma than in the epithelium, with higher metastasis-to-normal ratios (Figure 2 - Supplement 2-B and C); this can be explained by the low expression of KHSRP in the normal liver stroma. Comparison of matched primary tumor and liver metastasis (n=10 patients) showed that the expression of KHSRP is unchanged in the epithelial cells upon migration, however the metastatic stroma has a higher expression compared to the stroma in the primary tumor (Figure 2 - Supplement 2-D and E).

To validate the prognostic role of *KHSRP* in an independent cohort, we used a published dataset of 566 patients with stage I-IV CRC in the French Cartes d'Identité des Tumeurs program[36]. *KHSRP* expression was increased in tumor compared to uninvolved (*normal*) tissue, in accordance with our previous data (Figure 3-A). Survival analysis was restricted to stage II-III patients following recommendations from the original authors: high *KHSRP* expression was associated with a decreased 5-year relapse-free survival in this cohort (Figure 3-B, HR=1.95, 95% CI = 1.21-2.60, p=0.0038). *KHSRP* expression was not associated with other tumor features such as loss of mismatch repair (MMR) proteins, or mutations in *KRAS* or *BRAF* (Figure 3-C).

To independently validate the expression of KHSRP in epithelial and stromal compartments from the IHC data, we took advantage of a transcriptomic dataset of 13 CRC and normal colonic mucosa samples, in which epithelial cells and stromal cells had been microdissected by laser capture and profiled separately[37]. *KHSRP* was significantly

overexpressed in the microdissected epithelial tumor compared with tumor stromal areas, and to a lesser extent in the epithelium compared with the stroma of the normal colonic mucosa, in accordance with our IHC data (Figure 3-D). Although there was a trend in increased *KHSRP* expression in tumor versus normal tissue for both the epithelium and the stroma, these comparisons were not statistically significant probably due to the low number of samples. Finally, we used transcriptomic data from purified cell populations that were isolated from 14 dissociated human primary CRC samples[38]. Fluorescence-activated cell sorting (FACS) was used to enrich for epithelial cancer cells ($EpCAM^+$), leukocytes ($CD45^+$), endothelial cells ($CD31^+$) and cancer-associated fibroblasts (CAFs) (FAP^+). The expression of *KHSRP* was higher in the $Epcam^+$ epithelial cell population compared to the stromal cells, with the $CD31^+$ endothelial cells showing the lowest *KHSRP* expression (Figure 3-E).

KHSRP is involved in promoting the growth and survival of CRC cells

Next, we turned to an *in vitro* model of CRC to investigate the mechanistic role of KHSRP in epithelial cancer cells. We used the SW480 cell line, which was derived from a primary tumor of a moderately differentiated Duke B colon adenocarcinoma[39]. These cells constitutively express KHSRP with a diffuse intracellular pattern (Figure 4 – Supplement 1). An initial screen with a pool of 4 different siRNA sequences targeting *KHSRP* effectively silenced mRNA expression by 50% (Figure 4-A), and significantly reduced cell proliferation (Figure 4-B). We then confirmed and extended these initial results using an independent siRNA that effectively knocked down KHSRP protein expression (Figure 4-C): silencing of KHSRP reduced cell growth as measured by neutral red uptake (Figure 4-D), reduced clonogenic potential measured by both number of colonies (surviving fraction) and total colony area (Figure 4-E), and reduced spheroid formation in 3D Matrigel cultures (Figure 4-F). Similar results were obtained by silencing KHSRP in an independent cell line model, SW620, which was isolated from a lymph node after multiple metastases occurred in the same patient (Figure 4 - Supplement 2). Furthermore, we also developed a conditional (doxycycline-dependent) shRNA-based stable knockdown model from the SW620 cell line, which further confirmed results obtained with the transient silencing model (Figure 4 – Supplement 3).

KHSRP regulates cell cycle and affects the tumor-promoting microenvironment

To investigate the mechanisms involved in the tumor-promoting effects of KHSRP, we started by analyzing the transcriptomic profiles of siRNA-transfected KHSRP knockdown SW480 cells, compared to scramble control transfection (Figure 5 – Supplement 1). This preliminary analysis identified 135 genes differentially regulated upon KHSRP knockdown (Supplementary Table 3), which are enriched for functional categories related to cell growth and survival (specifically, cell cycle and apoptosis), as well as cell signaling and known KHSRP-related functions (translation, protein metabolism). This prompted us to investigate the effects of KHSRP knockdown on the cell cycle distribution of CRC cells. KHSRP siRNA caused an increase in the G0/G1 population (Figure 5-A), concomitant with a decrease in the mitotic index, measured as the number of cells positively stained by phospho-Histone H3 (Figure 5-B), indicative of a reduced proliferation rate due to a delayed G1/S transition. These data, together with that presented in Figure 4, suggest an involvement of KHSRP in driving epithelial cells into mitosis, thereby increasing proliferation.

Silencing of KHSRP gene expression did not change cell migration measured by a wound-healing assay, compared to non-targeting scramble control (Figure 6-A), and did not impact on the ability of CRC cells to invade through a Matrigel layer (Figure 6-B). However, the cell culture supernatant from cells transfected with KHSRP siRNA was able to reduce endothelial cell growth in a tube-forming assay (Figure 6-C), an indication that epithelial KHSRP expression could be involved in the secretion of specific extracellular signaling mediators promoting angiogenesis. In support of this, CRC cells with silenced KHSRP expression secreted reduced levels of IL-8 and VEGF (Figure 6-D).

KHSRP regulates the secretion of multiple proteins by tumor cells

To further investigate the involvement of KHSRP in regulating the extracellular microenvironment, we employed the conditional KHSRP knockdown cell line model (described in Figure 4 – Supplement 3) to probe the secretome of SW620 upon

doxycycline-induced, shRNA-mediated knockdown of KHSRP. Shotgun proteomics analysis identified 187 proteins, of which 42 where unique for the control samples (i.e. undetected in the doxycycline-treated samples), and 15 where unique for the doxycycline-treated samples (Figure 7-A). Statistical analysis of spectral counts data showed that most of proteins are downregulated upon doxycycline treatment, with 40 being significantly underexpressed or overexpressed by more than 50% (Figure 7-B, and Supplementary Table 4). GO term analysis of the 40 highly differentially regulated proteins revealed an enrichment for known terms related to KHSRP function (e.g. RNA binding, spliceosome) and expected terms related to the cellular location of the probed sample (e.g. membrane and extracellular space); interestingly, there was also a significant enrichment for terms related to the pro-tumorigenic extracellular microenvironment (e.g. exosomes, focal adhesion, cell migration), as well as terms broadly related to the immune response and specifically to myeloid cell activation (Figure 7-C). Specific examples of candidate proteins whose secretion is downregulated upon KHSRP knockdown included: the Rho-specific guanine nucleotide dissociation inhibitor α (RhoGDIα), a master regulator of Rho GTPases involved in promoting cell migration[40]; Quiescin sulfhydryl oxidase 1 (QSOX1), an enzyme involved in protein folding which promotes cell invasion by regulating the extra-cellular matrix at the tumor-stroma interface[41]; γ-Glutamyl hydrolase (GGH), a key regulator of folate homeostasis which is known to decrease chemosensitivity both *in vitro* and *in vivo*[42]. Conversely, a protein that is oversecreted in response to KHSRP knockdown is the actin-binding protein Villin-1, whose continuous down-regulation upon cellular stress induces intestinal epithelial cell death by necroptosis, accompanied by release of damage-associated molecular patterns (DAMPs) and intestinal inflammation[43].

DISCUSSION

The role of KHSRP in cancer, and specifically in the pathogenesis and progression of CRC has not been extensively studied. Here, we provide orthogonal evidence supporting a pro-tumorigenic role of KHSRP in CRC, based on extensive mining of multiple publicly available data sets, analysis of patient samples, as well as *in vitro* cell line models. We show by both WB and IHC that KHSRP is overexpressed at the protein level in primary tumors compared to adjacent normal tissue. We found that increased expression could be a potential indicator of negative clinical outcome. We further independently validated our data at the gene expression level using additional CRC cohorts from publicly available databases. Our findings agree with recent evidence for a tumor-promoting role of KHSRP in different indications, including osteosarcoma[20], lung cancer[19,44], esophageal squamous cell carcinoma[45].

KHSRP expression was not restricted to the epithelial compartment in CRC but was also detected in the stroma. Our IHC data from matched primary and metastatic tissue showed that expression of KHSRP remains unchanged in the epithelial cells upon liver infiltration, but stromal expression is strongly upregulated from a very low basal expression in the normal hepatic stroma. This suggests that invading epithelial cells are capable of modifying the local microenvironment at the secondary site, or alternatively that a local increase in KHSRP expression is pre-existing and might even contribute to the metastatic niche[46]. In fact, KHSRP is involved in the transient expression of the chemokine CX3CL1 in liver epithelial cells in response to IFN-γ stimulation[47], contributing to the control of cellular homeostasis during inflammation and macrophage infiltration.

To further investigate the role of KHSRP at the molecular level, we used a loss-of-function approach in two cell line models of CRC (SW480 and SW620), which originated from the primary tumor and lymph node metastasis of the same patient (respectively) and are an ideal model to study tumor progression. Our *in vitro* data recapitulates what was seen *ex vivo*, supporting a role of KHSRP in driving epithelial cell proliferation in both the primary and metastatic setting. Mechanistically, we showed that KHSRP regulates cell cycle by driving cells through G1/S transition, and we provided

preliminary evidence by gene-expression microarray of possible alternative mechanisms involving control of transcription, protein synthesis and multiple cell signaling pathways. We also reported novel data suggesting that KHSRP could be involved in regulating the tumor microenvironment, with implications for tumor progression and metastasis. Specifically, epithelial KHSRP was involved in promoting a pro-angiogenic extracellular environment, as well as regulating the secretion of oncogenic proteins involved in diverse cellular processes such as migration and response to cellular stress. To the best of our knowledge, this represents the first report of such an effect for KHSRP in shaping the extracellular environment of epithelial cells. Although preliminarily, our data also suggest a possible role for KHSRP in regulating immune response genes, both at the gene-expression level and at the secretome level (as reported by microarray and proteomic data). This suggests the intriguing idea that the reported negative prognostic role of KHSRP could be partly ascribed to a regulation of immune evasion mechanisms, and provides a rationale for reconciling the oncogenic roles of KHSRP with its other known functions in shaping innate immunity during viral infection and inflammation. In fact, recent work from Bezzi *et al.* using genetically engineered mouse models of prostate cancer driven by the loss of specific tumor suppressor genes has shown that the genetic landscape of epithelial tumor cells can directly influence the composition of immune cell infiltrates in primary tumors, through mechanisms based on distinct chemokine pools resulting from aberrant transcriptional and signaling programs[48]. Furthermore, knockout mice studies have shown a requirement of KHSRP for the post-transcriptional control of type-1 IFN genes[13]. Recent mechanistic evidence proved that KHSRP can directly associate and negatively regulate retinoic acid-inducible gene I (RIG-I) receptor signaling during viral infection; this exert a negative control on the activation of type-I IFN innate immune responses during the recognition of pathogen-associated molecular patterns (PAMPs) encoded by viral RNA[49]. This could have potential consequences for the control of anti-tumor innate immune responses, as similar mechanisms are involved in the recognition of damage-associated molecular pattern (DAMPs) and the immunogenicity of tumor cells[50].

There is also considerable interest in the suitability of different members of the translational control machinery as potential therapeutic targets in cancer, although the

evidence so far is almost entirely at the preclinical stage[2]. Small molecule inhibition of the RBP HuR in APC^{Min} mice led to a 25% reduction in small intestinal tumor formation, and a concomitant reduction in c-myc protein levels[51]. Another recent report showed that inhibition of mTORC1 using rapamycin caused regression of established APC-deficient intestinal tumors, suggesting that inhibition of translation elongation using existing clinically approved drugs could provide therapeutic benefit for patients at high risk of developing CRC[52]. Our loss-of-function data in *in vitro* CRC models suggest that KHSRP could also have putative therapeutic implications and warrants further investigation into the suitability of such an approach.

In conclusion, our report sheds light onto the molecular role of KHSRP in colorectal carcinogenesis, providing for the first time comprehensive data in support of a novel pro-tumorigenic role of this RBP in the gut through direct modulation of epithelial cell phenotype and indirect modulation of the tumor microenvironment.

Acknowledgments

We gratefully acknowledge Dr. Giselle Knudsen (UCSF), Dr. Sudipto Das (RCSI), Dr. Janet McCormack (UCD), Dr. Barry Moran (TCD), and Dr. Dimitri Scholz (UCD) for technical assistance at various stages of this project. We also wish to thank Dr. Martin Kampmann (UCSF) for providing advice and material for the generation of the conditional knockdown cell lines, and Dr. Quing Xiong (Southwest University, Chongqing, China) for providing access to their data. The bioinformatic expertise of Dr. Tim Hacker and Sam Ivry (UCSF) is also acknowledged. Mass spectrometry was performed in collaboration with the UCSF Mass Spectrometry Facility (directed by Prof. Alma Burlingame).

References

1. Hanahan D, Weinberg RA. Hallmarks of cancer: the next generation. *Cell*. 2011;144(5):646–674. doi:10.1016/j.cell.2011.02.013.

2. Silvera D, Formenti SC, Schneider RJ. Translational control in cancer. *Nature Reviews Cancer*. 2010;10(4):254–266. doi:10.1038/nrc2824.

3. Truitt ML, Ruggero D. New frontiers in translational control of the cancer genome. *Nature Reviews Cancer*. 2016;16(5):288–304. doi:10.1038/nrc.2016.27.

4. Gerstberger S, Hafner M, Tuschl T. A census of human RNA-binding proteins. *Nat Rev Genet*. 2014;15(12):829–845. doi:10.1038/nrg3813.

5. Briata P, Chen C-Y, Ramos A, Gherzi R. Functional and molecular insights into KSRP function in mRNA decay. *Biochim Biophys Acta*. 2013;1829(6-7):689–694. doi:10.1016/j.bbagrm.2012.11.003.

6. Gherzi R, Lee K-Y, Briata P, et al. A KH Domain RNA Binding Protein, KSRP, Promotes ARE-Directed mRNA Turnover by Recruiting the Degradation Machinery. *Mol Cell*. 2004;14(5):571–583. doi:10.1016/j.molcel.2004.05.002.

7. Chou CF, Mulky A, Maitra S, et al. Tethering KSRP, a Decay-Promoting AU-Rich Element-Binding Protein, to mRNAs Elicits mRNA Decay. *Mol Cell Biol*. 2006;26(10):3695–3706. doi:10.1128/MCB.26.10.3695-3706.2006.

8. Dhamija S, Kuehne N, Winzen R, et al. Interleukin-1 activates synthesis of interleukin-6 by interfering with a KH-type splicing regulatory protein (KSRP)-dependent translational silencing mechanism. *J Biol Chem*. 2011;286(38):33279–33288. doi:10.1074/jbc.M111.264754.

9. Trabucchi M, Briata P, Garcia-Mayoral M, et al. The RNA-binding protein KSRP promotes the biogenesis of a subset of microRNAs. *Nature*. 2009;459(7249):1010–1014. doi:10.1038/nature08025.

10. Guo L, Zaysteva O, Nie Z, et al. Defining the essential function of FBP/KSRP proteins: Drosophila Psi interacts with the mediator complex to modulate MYC transcription and tissue growth. *Nucleic Acids Res*. May 2016. doi:10.1093/nar/gkw461.

11. Winzen R, Thakur BK, Dittrich-Breiholz O, et al. Functional analysis of KSRP interaction with the AU-rich element of interleukin-8 and identification of inflammatory mRNA targets. *Mol Cell Biol*. 2007;27(23):8388–8400. doi:10.1128/MCB.01493-07.

12. Gherzi R, Chen C-Y, Ramos A, Briata P. KSRP controls pleiotropic cellular functions. *Semin Cell Dev Biol*. 2014;34:2–8. doi:10.1016/j.semcdb.2014.05.004.

13. Lin W-J, Zheng X, Lin C-C, et al. Posttranscriptional control of type I interferon genes by KSRP in the innate immune response against viral infection. *Mol Cell Biol*. 2011;31(16):3196–3207. doi:10.1128/MCB.05073-11.

14. Suswam EA, Nabors LB, Huang Y, Yang X, King PH. IL-1beta induces stabilization of IL-8 mRNA in malignant breast cancer cells via the 3' untranslated region: Involvement of divergent RNA-binding factors HuR, KSRP and TIAR. *Int J Cancer*. 2005;113(6):911–919. doi:10.1002/ijc.20675.

15. Giovarelli M, Bucci G, Pasero M, Gherzi R, Briata P. KSRP silencing favors neural differentiation of P19 teratocarcinoma cells. *Biochim Biophys Acta*. 2013;1829(5):469–479. doi:10.1016/j.bbagrm.2013.02.008.

16. Santarosa M, Del Col L, Viel A, et al. BRCA1 modulates the expression of hnRNPA2B1 and KHSRP. *Cell Cycle*. 2010;9(23):4666–4673.

17. Walerych D, Lisek K, Sommaggio R, et al. Proteasome machinery is instrumental in a common gain-of-function program of the p53 missense mutants in cancer. *Nat Cell Biol*. 2016;18(8):897–909. doi:10.1038/ncb3380.

18. Puppo M, Bucci G, Rossi M, et al. miRNA-Mediated KHSRP Silencing Rewires Distinct Post-transcriptional Programs during TGF-β-Induced Epithelial-to-Mesenchymal Transition. *Cell Rep*. 2016;16(4):967–978. doi:10.1016/j.celrep.2016.06.055.

19. Tong L, Luo Y, Wei T, et al. KH-type splicing regulatory protein (KHSRP) contributes to tumorigenesis by promoting miR-26a maturation in small cell lung cancer. *Mol Cell Biochem*. 2016;422(1-2):61–74. doi:10.1007/s11010-016-2806-y.

20. Pruksakorn D, Teeyakasem P, Klangjorhor J, et al. Overexpression of KH-type splicing regulatory protein regulates proliferation, migration, and implantation ability of osteosarcoma. *Int J Oncol*. 2016;49(3):903–912. doi:10.3892/ijo.2016.3601.

21. Wurth L, Gebauer F. RNA-binding proteins, multifaceted translational regulators in cancer. *Biochim Biophys Acta*. 2015;1849(7):881–886. doi:10.1016/j.bbagrm.2014.10.001.

22. Fagoonee S, Picco G, Orso F, et al. The RNA-binding protein ESRP1 promotes human colorectal cancer progression. *Oncotarget*. 2017;8(6):10007–10024. doi:10.18632/oncotarget.14318.

23. Blanc V, Henderson JO, Newberry RD, et al. Deletion of the AU-rich RNA binding protein Apobec-1 reduces intestinal tumor burden in Apc(min) mice. *Cancer Research*. 2007;67(18):8565–8573. doi:10.1158/0008-5472.CAN-07-1593.

24. Sureban SM, May R, George RJ, et al. Knockdown of RNA Binding Protein Musashi-1 Leads to Tumor Regression In Vivo. *Gastroenterology*.

2008;134(5):1448–1458.e2. doi:10.1053/j.gastro.2008.02.057.

25. Wang S, Li N, Yousefi M, et al. Transformation of the intestinal epithelium by the MSI2 RNA-binding protein. *Nat Commun*. 2015;6:6517. doi:10.1038/ncomms7517.

26. Preitner N, Quan J, Nowakowski DW, et al. APC is an RNA-binding protein, and its interactome provides a link to neural development and microtubule assembly. *Cell*. 2014;158(2):368–382. doi:10.1016/j.cell.2014.05.042.

27. Peng L, Bian X-W, Li DK, et al. Large-scale RNA-Seq Transcriptome Analysis of 4043 Cancers and 548 Normal Tissue Controls across 12 TCGA Cancer Types. *Sci Rep*. 2015;5:13413. doi:10.1038/srep13413.

28. Gao J, Aksoy BA, Dogrusoz U, et al. Integrative Analysis of Complex Cancer Genomics and Clinical Profiles Using the cBioPortal. *Science Signaling*. 2013;6(269):pl1–pl1. doi:10.1093/bioinformatics/btq430.

29. Noonan SA, Morrissey ME, Martin P, et al. Tumour vasculature immaturity, oxidative damage and systemic inflammation stratify survival of colorectal cancer patients on bevacizumab treatment. *Oncotarget*. 2018;5(0). doi:10.18632/oncotarget.24276.

30. Detre S, Saclani Jotti G, Dowsett M. A “quickscore” method for immunohistochemical semiquantitation: validation for oestrogen receptor in breast carcinomas. *J Clin Pathol*. 1995;48(9):876–878.

31. Repetto G, del Peso A, Zurita JL. Neutral red uptake assay for the estimation of cell viability/cytotoxicity. *Nat Protoc*. 2008;3(7):1125–1131. doi:10.1038/nprot.2008.75.

32. Lee GY, Kenny PA, Lee EH, Bissell MJ. Three-dimensional culture models of normal and malignant breast epithelial cells. *Nat Methods*. 2007;4(4):359–365. doi:10.1038/nmeth1015.

33. Hong Y, Downey T, Eu KW, Koh PK, Cheah PY. A “metastasis-prone” signature for early-stage mismatch-repair proficient sporadic colorectal cancer patients and its implications for possible therapeutics. *Clin Exp Metastasis*. 2010;27(2):83–90. doi:10.1007/s10585-010-9305-4.

34. Cancer Genome Atlas Network. Comprehensive molecular characterization of human colon and rectal cancer. *Nature*. 2012;487(7407):330–337. doi:10.1038/nature11252.

35. Ki DH, Jeung H-C, Park CH, et al. Whole genome analysis for liver metastasis gene signatures in colorectal cancer. *Int J Cancer*. 2007;121(9):2005–2012. doi:10.1002/ijc.22975.

36. Marisa L, de Reyniès A, Duval A, et al. Gene expression classification of colon cancer into molecular subtypes: characterization, validation, and prognostic value. *PLoS Med*. 2013;10(5):e1001453. doi:10.1371/journal.pmed.1001453.

37. Nishida N, Nagahara M, Sato T, et al. Microarray analysis of colorectal cancer stromal tissue reveals upregulation of two oncogenic miRNA clusters. *Clinical Cancer Research*. 2012;18(11):3054–3070. doi:10.1158/1078-0432.CCR-11-1078.

38. Calon A, Espinet E, Palomo-Ponce S, et al. Dependency of colorectal cancer on a TGF-β-driven program in stromal cells for metastasis initiation. *Cancer Cell*. 2012;22(5):571–584. doi:10.1016/j.ccr.2012.08.013.

39. Leibovitz A, Stinson JC, McCombs WB, McCoy CE, Mazur KC, Mabry ND. Classification of human colorectal adenocarcinoma cell lines. *Cancer Research*. 1976;36(12):4562–4569.

40. Zhao L, Wang H, Li J, Liu Y, Ding Y. Overexpression of Rho GDP-Dissociation Inhibitor Alpha Is Associated with Tumor Progression and Poor Prognosis of Colorectal Cancer. *Journal of proteome research*. 2008;7(9):3994–4003. doi:10.1021/pr800271b.

41. Katchman BA, Antwi K, Hostetter G, et al. Quiescin Sulfhydryl Oxidase 1 Promotes Invasion of Pancreatic Tumor Cells Mediated by Matrix Metalloproteinases. *Molecular Cancer Research*. 2011;9(12):1621–1631. doi:10.1158/1541-7786.MCR-11-0018.

42. Kim S-E, Cole PD, Cho RC, et al. γ-Glutamyl hydrolase modulation and folate influence chemosensitivity of cancer cells to 5-fluorouracil and methotrexate. *British Journal of Cancer*. 2013;109(8):2175–2188. doi:10.1074/jbc.M002580200.

43. Roy S, Esmaeilniakooshkghazi A, Patnaik S, et al. Villin-1 and Gelsolin Regulate Changes in Actin Dynamics That Affect Cell Survival Signaling Pathways and Intestinal Inflammation. *Gastroenterology*. December 2017. doi:10.1053/j.gastro.2017.12.016.

44. Bikkavilli RK, Zerayesus SA, Van Scoyk M, et al. KSRP promotes post-transcriptional destabilization of Spry4 transcripts in non-small cell lung cancer. *J Biol Chem*. March 2017. doi:10.1074/jbc.M116.757906.

45. Fujita Y, Masuda K, Hamada J, et al. KH-type splicing regulatory protein is involved in esophageal squamous cell carcinoma progression. *Oncotarget*. 2017;8(60):101130–101145. doi:10.18632/oncotarget.20926.

46. Descot A, Oskarsson T. The molecular composition of the metastatic niche. *Exp Cell Res*. 2013;319(11):1679–1686. doi:10.1016/j.yexcr.2013.04.017.

47. Xia Z, Lu Y, Li X, Mao T, Chen X-M, Zhou R. Upregulation of KSRP by miR-27b provides IFN-γ-induced post-transcriptional regulation of CX3CL1 in liver

epithelial cells. *Sci Rep*. 2015;5:17590. doi:10.1038/srep17590.

48. Bezzi M, Seitzer N, Ishikawa T, et al. Diverse genetic-driven immune landscapes dictate tumor progression through distinct mechanisms. *Nat Med*. 2018;24(2):165–175. doi:10.1158/2159-8290.CD-12-0095.

49. Soonthornvacharin S, Rodriguez-Frandsen A, Zhou Y, et al. Systems-based analysis of RIG-I-dependent signalling identifies KHSRP as an inhibitor of RIG-I receptor activation. *Nat Microbiol*. 2017;2:17022. doi:10.1038/nmicrobiol.2017.22.

50. Green DR, Ferguson T, Zitvogel L, Kroemer G. Immunogenic and tolerogenic cell death. *Nat Rev Immunol*. 2009;9(5):353–363. doi:10.1038/nri2545.

51. Lang M, Berry D, Passecker K, et al. HuR small molecule inhibitor elicits differential effects in adenomatosis polyposis and colorectal carcinogenesis. *Cancer Research*. January 2017:canres.1726.2015. doi:10.1158/0008-5472.CAN-15-1726.

52. Faller WJ, Jackson TJ, Knight JRP, et al. mTORC1-mediated translational elongation limits intestinal tumour initiation and growth. *Nature*. 2015;517(7535):497–500. doi:10.1038/nature13896.

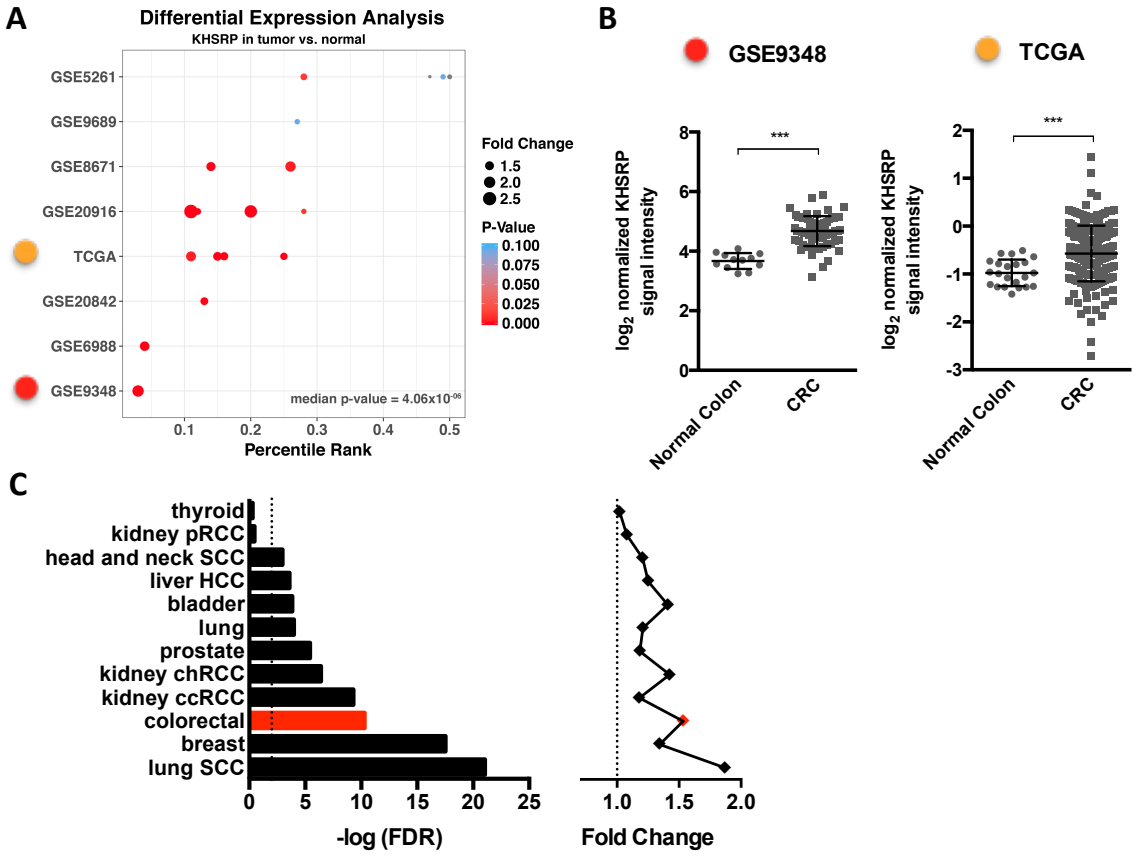

Figure 1: *In silico* analysis of publicly available CRC datasets reveals a consistent tumor-specific over-expression of KHSRP. **(A)** Differential expression analysis of KHSRP in the Oncomine database returns 18 analyses (each comprising a different patient group compared to normal tissue) across 8 different CRC datasets. The analyses are plotted by percentile ranking of KHSRP over-expression (as a percentage of all overexpressed genes in the dataset); dots are sized in proportion to the fold change of KHSRP expression in tumor vs. normal, and colored by p-value (further details of the analyses are provided in supplementary table 1). **(B)** Differential expression of KHSRP between tumor and normal tissue showing individual data points is reported for the two representative analyses indicated (with the color code referring to panel A). *** $p<0.0001$ (Mann-Whitney test). **(C)** Differential expression analysis for KHSRP in RNA-Seq data for the indicated 12 cancer types in the TCGA dataset. For each type, the fold change expression of KHSRP in tumor versus normal tissue and the associated FDR-adjusted p-value are reported.

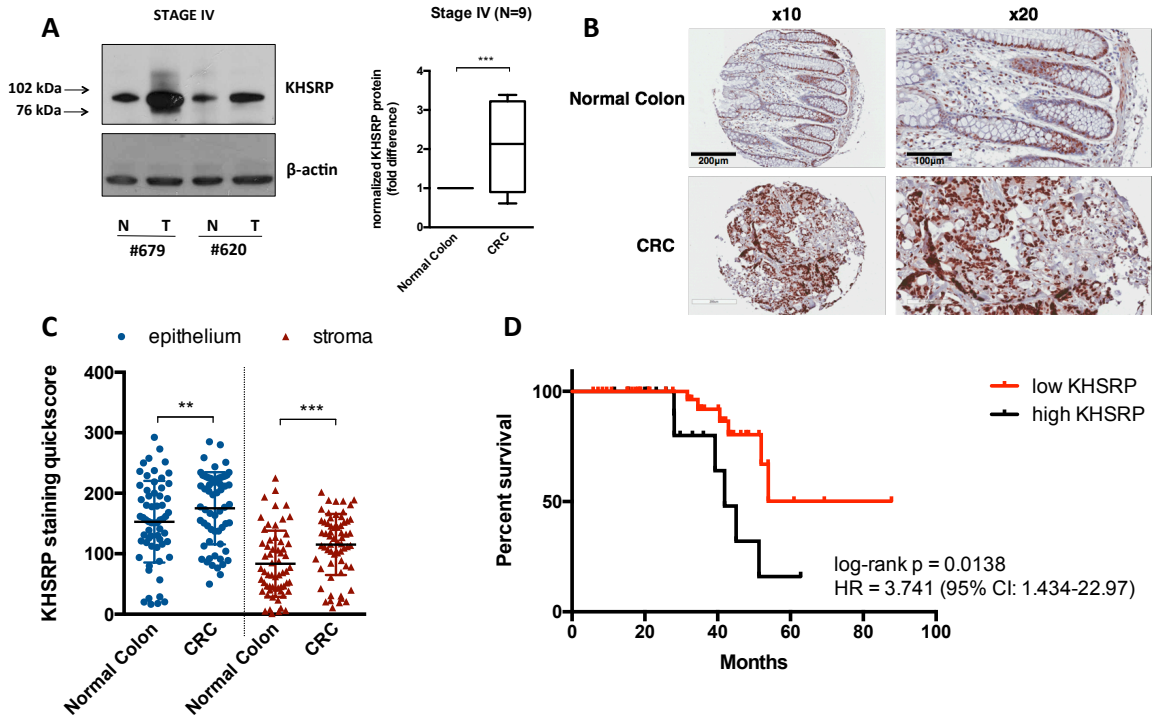

Figure 2: Analysis of KHSRP expression in primary tissue samples reveals a tumor-specific overexpression with prognostic value. **(A)** Western blot analysis of KHSRP in lysates from fresh-frozen tissue samples of patients with stage IV CRC (N=9), comparing tumor (T) and matched normal tissue (N) from each patient. A representative blot for 2 patients is shown along with semi-quantitative densitometric analysis of all patients. ***p<0.0001 (Student's *t* test) **(B)** Representative images from TMA sections of normal and CRC tissue stained for KHSRP. **(C)** Quantitation of stromal and epithelial KHSRP staining in normal colon vs. primary CRC tissue samples from the TMA. ** p<0.01 and ***p<0.0001 (Wilcoxon). **(D)** T/N ratios in the epithelium were used to segregate patients, using 20% as a cutoff (T/N<1.2 versus T/N>1.2). Survival curves were calculated according to the Kaplan–Meier method and compared using the Cox–Mantel log-rank test. The hazard ratio (HR) and associated confidence interval are shown.

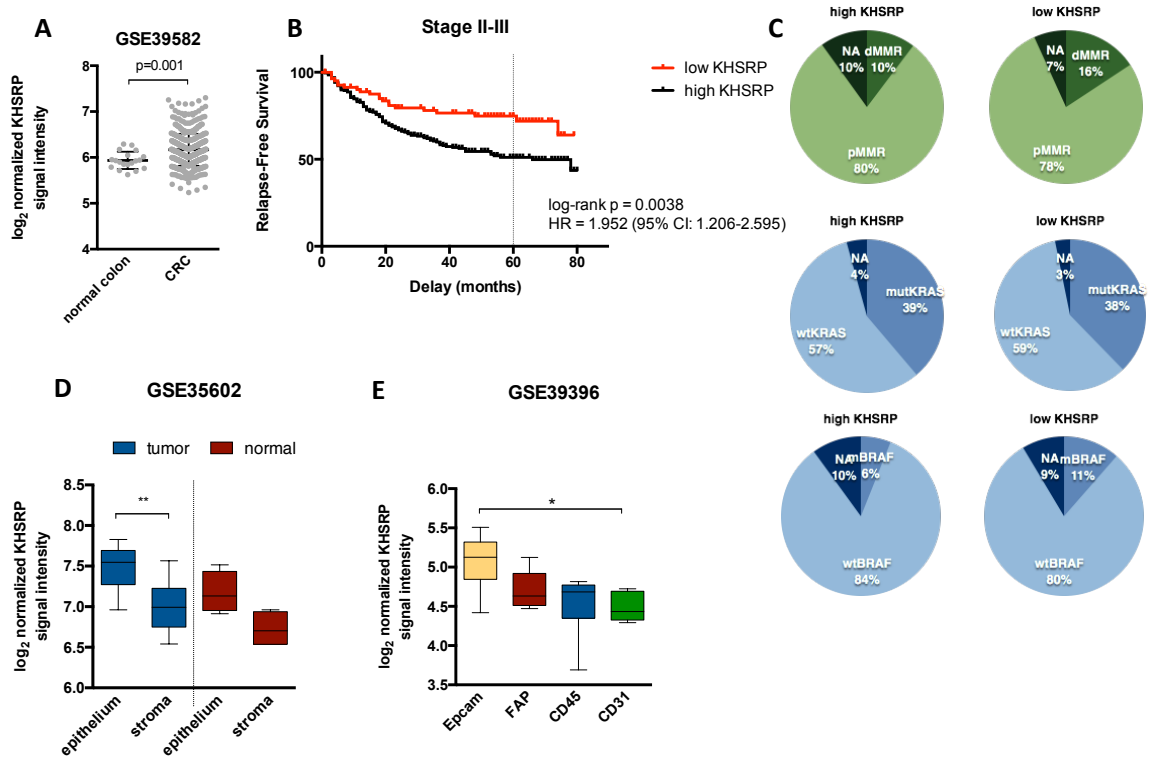

Figure 3: in silico analysis of three independent cohorts validates the overexpression and prognostic significance of KHSRP. **(A)** Log_2 normalized signal intensity of *KHSRP* in a cohort of 566 CRC patients and 19 normal controls profiled by gene expression microarrays [36] (Mann-Whitney test). **(B)** Survival curves for patients segregated into high/low groups using the 25th percentile of the *KHSRP* probe signal intensity. The hazard ratio (HR) and associated confidence interval are shown. **(C)** Distribution of patients with high/low *KHSRP* expression according to clinical characteristics: mismatch repair deficient (dMMR, i.e. MSI) or proficient (pMMR, i.e. MSS), KRAS (codon 12 and 13) mutational status, BRAF (p.V600E) mutational status. **(D)** Expression of *KHSRP* in laser-capture microdissected epithelial and stromal cells from 13 CRC and normal colonic mucosa samples [37]. ** $p<0.01$ (Kruskal-Wallis) **(E)** Expression of *KHSRP* in a cohort of FACS-sorted cells from 14 CRC patients. EpCAM: epithelial cancer cells; CD45: leukocytes; CD31: endothelial cells; FAP: cancer-associated fibroblasts. *$p<0.05$ (Kruskal-Wallis)

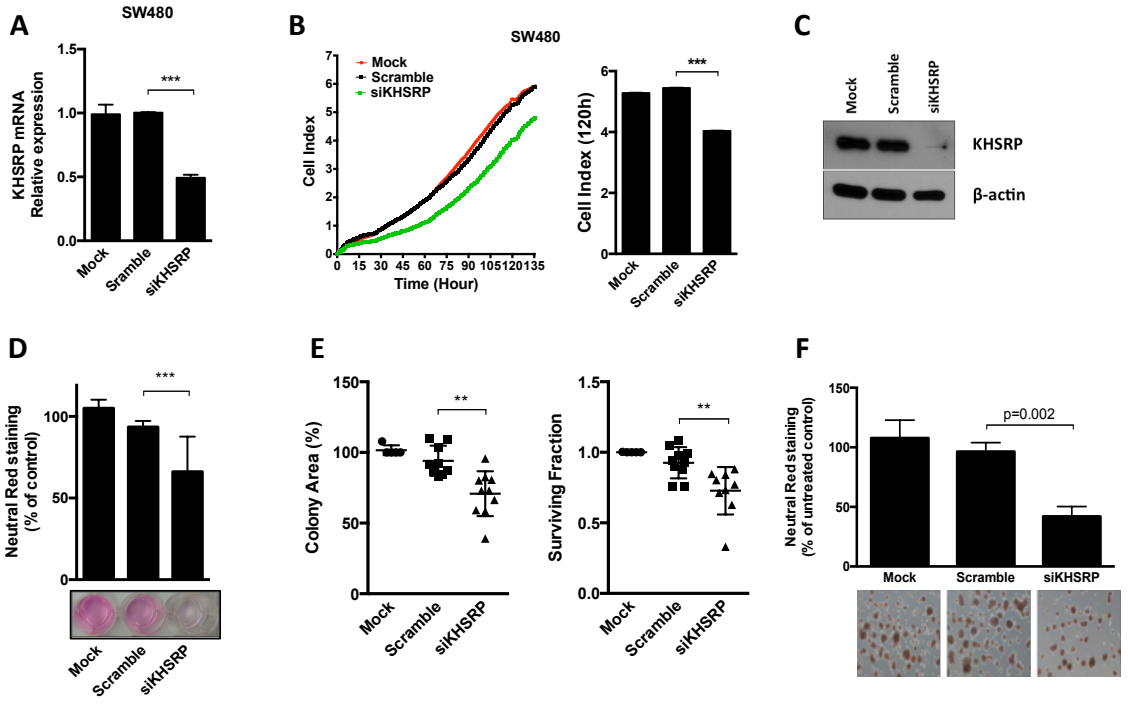

Figure 4: KHSRP is involved in growth and survival of an *in vitro* CRC cell line model. **(A)** qRT-PCR analysis of SW480 cells transfected with a pool of siRNAs targeting *KHSRP* or a scramble control pool for 48h. **(B)** Continuous monitoring of proliferation of siRNA pool-transfected cells; full time-course curves are shown, along with differences in cell index values after 5 days. ***p<0.0001 (ANOVA). **(C)** WB analysis of KHSRP protein expression in SW480 cells transfected with an siRNA targeting *KHSRP*, or a scramble control siRNA, or a mock transfection control for 48h. **(D)** Growth of transfected cells monitored after 7 days by neutral red assay; representative images are shown with staining quantification from triplicate assays. **(E)** Clonogenic potential for the transfected cells measured by both colony area and surviving fraction. **(F)** Spheroids from transfected cells grown in Matrigel; representative images are shown with staining quantification from triplicate assays. **p<0.001, and ***p<0.0001 (ANOVA).

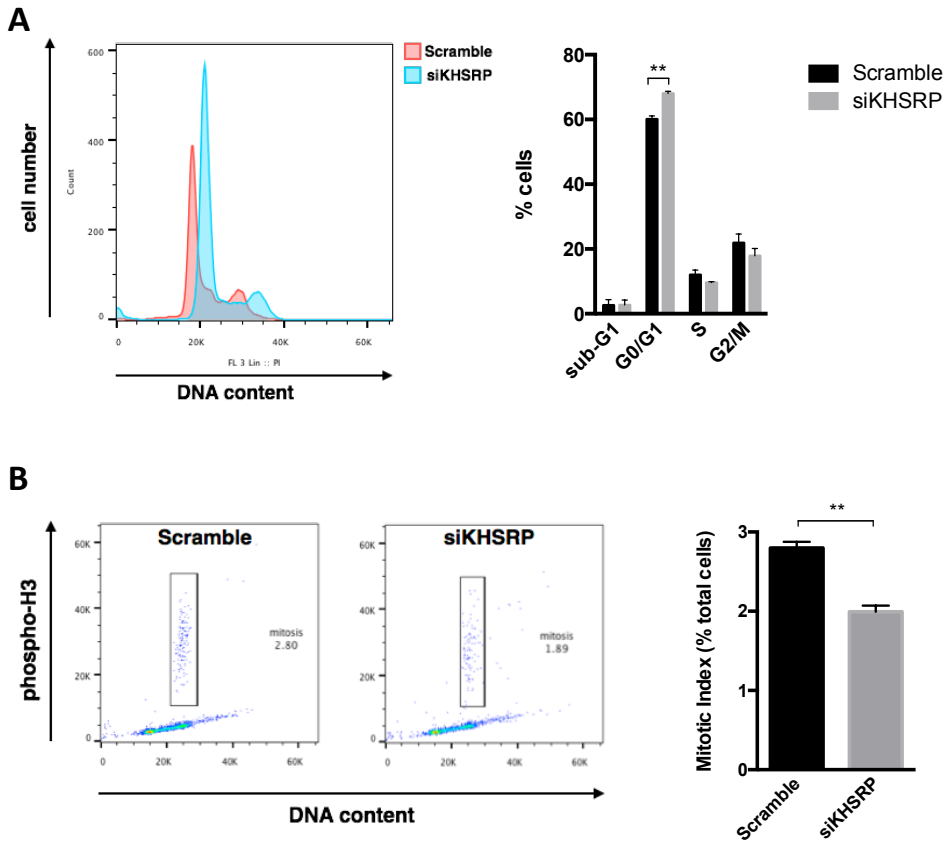

Figure 5: KHSRP is involved in regulating cell cycle and mitosis *in vitro*. **(A)** Cell cycle analysis of SW480 cells transfected with siKHSRP or Scramble negative control siRNA; a representative histogram of propidium iodide staining from one experiment is shown, along with a bar graph of cell distribution into cell cycle phases across three replicate experiments. **p<0.001 (ANOVA) **(B)** Analysis of mitotic cells by quantitation of phosphor-histone H3 in transfected SW480; a representative histogram is shown with bar graph of three replicate experiments. **p<0.001 (Mann-Whitney).

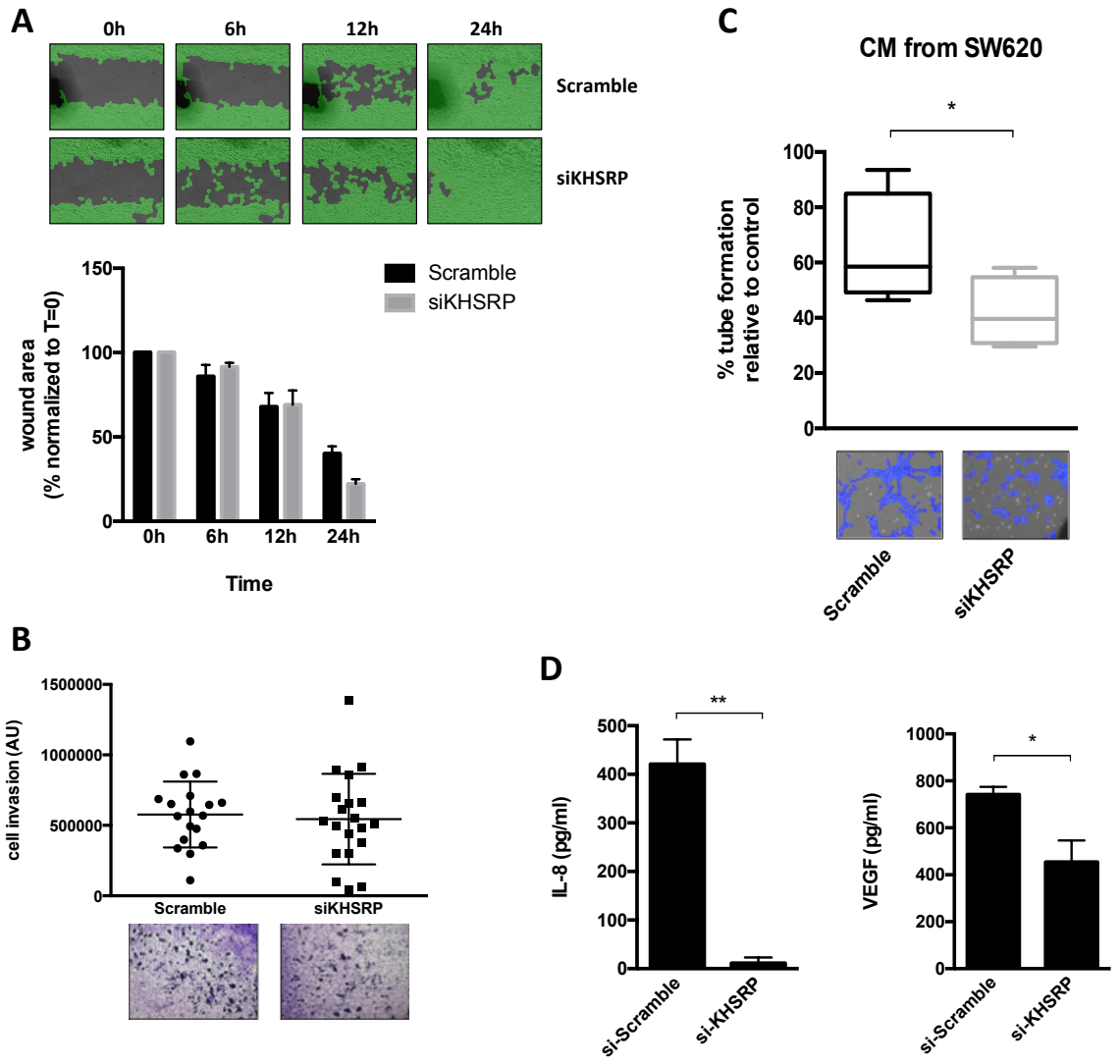

Figure 6: KHSRP does not impact on cell motility but influences the pro-tumorigenic extracellular environment. **(A)** Wound-healing assay of SW480 cells transfected with siKHSRP or Scramble negative control siRNA; representative images from one experiment are shown, with quantitation of wound area from two replicate experiments. **(B)** Invasion of SW620 cells transfected with siKHSRP or Scramble negative control siRNA, measured by the capacity to migrate through Matrigel; quantification of invaded cells from three replicate experiments is shown, along with representative images. **(C)** Endothelial tube formation of HDEC cells treated with conditioned media (CM) from SW620 cells transfected as above. *$p<0.05$ (Student's *t* test). **(D)** Expression of secreted IL-8 and VEGF in the CM of SW620 cells transfected as above, measured by ELISA. *$p<0.05$, **$p<0.001$ (Student's *t* test).

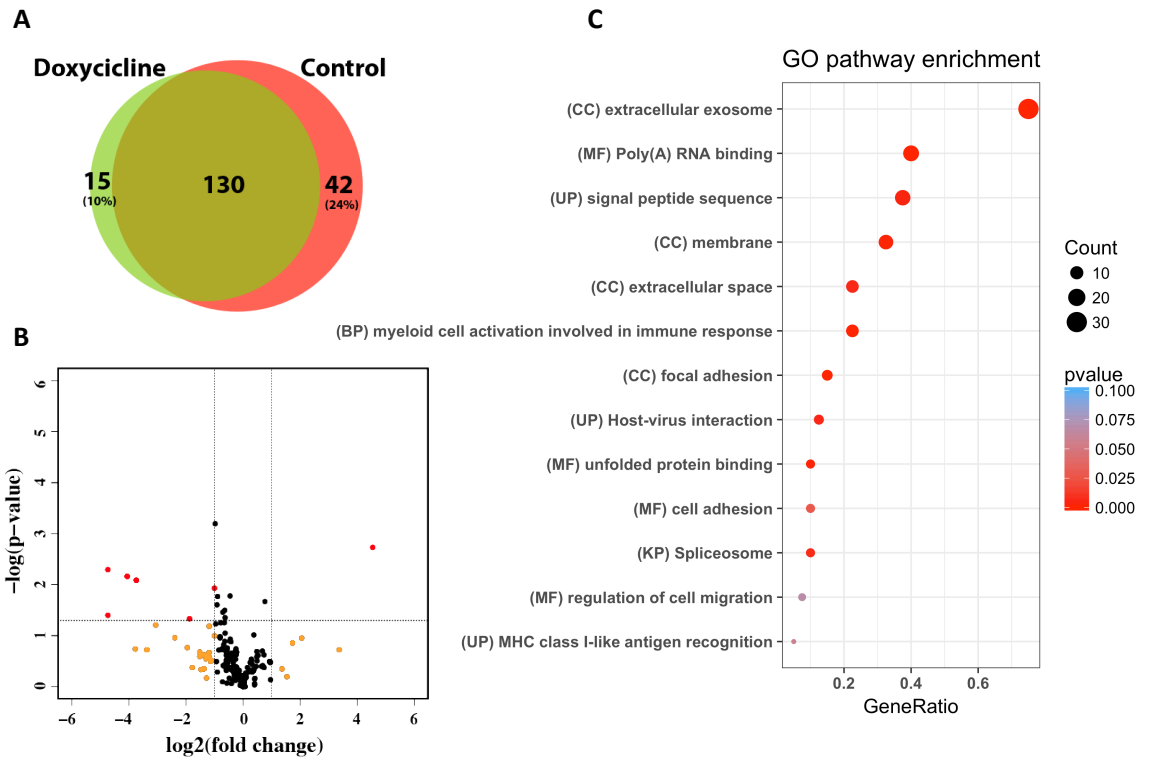

Figure 7: KHSRP regulates expression of key proteins that modulate the tumorigenic microenvironment. Differential expression of secreted proteins in conditioned media from SW620 cells treated with Doxycicline for 4 days to induce shRNA-mediated KHSRP knockdown. Conditioned media was analyzed by shotgun proteomics. **(A)** Venn diagram depicting shared and unique proteins identified in triplicate LC-MS/MS experiments for each condition. **(B)** Volcano plot showing differentially regulated proteins in the doxycycline-treated samples compared to control, colored in red ($\log_2$ Fold Change > |1|, p-value < 0.05). Proteins that are differentially regulated above the fold change threshold with a non-significant p-value are colored in yellow **(C)** Dot plot of results from a GO analysis of the 40 highly differentially regulated proteins. GO terms are reported with their category (CC=cellular component, MF=molecular function, BP=biological process, UP=uniprot annotation, KP=Kegg pathway) and plotted by gene ratio (the number of genes in one GO term compared to the total). Dots are sized in proportion to the number of hits within a GO term, and colored by p-value.

Table 1: Summary of clinical characteristics for the patients included in the two cohorts analyzed by either Western blotting (WB) or Tissue Microarrays (TMA).

TABLE 1: clinical characteristics of CRC patients		
Variable	**Number of Patients (%)**	
	WB cohort	**TMA cohort**
Total Patients	16	62
Tissue Type	fresh frozen	FFPE
Age mean (range)	65.8 (50-82)	63.5 (25-84)
Gender		
M	9	34
F	7	28
Dukes stage		
A	0	1
B	8	12
C	7	24
D	1	25
KRAS		
wild-type	5	N/A
mutant	4	N/A
Microsatellite		
MSI	1	N/A
MSS	15	N/A
Location		
Right	10	N/A
Left	6	N/A